Antigen targeting to Fc receptors on dendritic cells : implications for T lymphocyte-directed immunotherapy

Montfoort, A.G. van

Antigen Storage Compartments in Mature Dendritic Cells Facilitate Prolonged CTL Cross-Priming Capacity

Nadine van Montfoort, Marcel G. Camps, Selina Khan, Dmitri V. Filippov, Jimmy J. Weterings, Janice M. Griffith, Hans J. Geuze, Thorbald van Hall, J. Sjef Verbeek, Cornelis J. Melief and Ferry Ossendorp

Published in Proceedings of the National Academy of Sciences of the United States of America, 2009; 106:6730-6735

Chapter 6

Abstract

Dendritic cells (DCs) are crucial for priming of naïve $CD8^+$ T lymphocytes to exogenous antigens, so called cross-priming. We report that exogenous protein antigen can be conserved for several days in mature DCs, coinciding with strong CTL cross-priming potency *in vivo*. After MHC class I peptide elution, protein antigen-derived peptide presentation is efficiently restored, indicating the presence of an intracellular antigen depot. We characterized this depot as a lysosome-like organelle, distinct from MHC class II compartments and recently described early endosomal compartments that allow acute antigen presentation in MHC class I. The storage compartments we report here facilitate continuous supply of MHC class I ligands. This mechanism ensures sustained cross-presentation by DCs, despite the short-lived expression of MHC class I/peptide complexes at the cell surface.

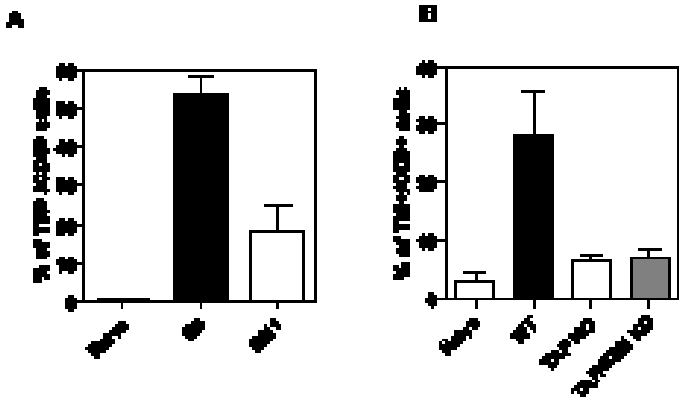

Supplementary Figure 2

(A) Induction of OVA-specific CTL in WT recipient mice (n=4) that were not injected (naïve), or injected i.v. with BM DC derived from B6 WT mice (black bars) or bm1 mice (white bars) pulse-loaded for one hour with IgG-OVA and subsequently cultured for 48 hours in the absence of antigen, measured by tetramer analysis. Error bar represents standard error of the mean (SEM). (B) Induction of OVA-specific CTL in WT recipient mice (n=5) that were not injected (naïve), or injected i.v. with BM DC derived from WT mice (black bars), transporter associated with antigen processing (TAP) deficient mice (white bars, TAP KO) or TAP/β2M deficient mice (white bars, TAP/ β2M KO), pulse-loaded for one hour with IgG-OVA and subsequently cultured for 48 hours in the absence of antigen, measured by tetramer analysis. Error bar represents SEM. Equal uptake of IgG-OVA and upregulation of co-stimulatory molecules CD40 and CD86 by all BM DCs after 48 hrs culture was verified by flow cytometry (data not shown). In both models, T cell induction was largely abrogated by BM DCs that were not capable of MHC class I presentation of the antigenic peptide. These experiments indicate that injected DCs directly induce antigen-specific $CD8^+$ T cells while antigen transfer to other APC plays a negligible role in the CTL cross-priming we have observed.

Introduction

Dendritic cells (DCs) are crucial in the initiation and orchestration of the T cell immune response (1-3). DCs operate as sentinels of an infection in the periphery and subsequently as conductors of the T cell response in the lymph nodes. To exert these functions, DCs are specialized in the ingestion, processing and presentation of antigens acquired by receptor independent pinocytosis or by receptor-mediated endocytosis (4-6). To this end they are equipped with a diverse set of receptors for uptake of antigen, such as scavenger receptors, lectin receptors or IgG (Fcγ) receptors (7).

Immature DCs have the capacity to efficiently acquire antigen, but a poor capacity to migrate and to stimulate T cells. Proper T cell response initiation requires maturation of the DCs, a process that is triggered by contact with infectious or inflammatory signals. Mature DC characteristically show enhanced migratory capacity, up-regulation of the MHC class I processing machinery and enhanced expression of MHC I and II and co-stimulatory molecules.

DCs present antigenic peptides in either MHC class I to induce CD8 T cell responses and in MHC class II to induce CD4 T cell responses. While MHC class I ligands are commonly derived from breakdown products of endogenous proteins that are degraded by the proteasome (8), DCs also have the unique capacity to present peptides derived from exogenous antigens in MHC class I to $CD8^+$ T cells, a process called "cross-presentation". This process is crucial for induction of effective CTL immunity against tumors, which lack direct priming capacity themselves, but also against micro-organisms including viruses (1).

DCs have dedicated organelles to facilitate efficient loading of antigenic peptides in MHC class II molecules. These MHC class II compartments (MIIC) are multi-vesicular endosomes that express high levels of MHC class II and invariant chain and are abundantly present in immature DCs (9). Upon maturation of the DC, rapid reorganisation of the MIIC takes place that facilitates transport of MHC class II molecules loaded with peptide to the cell surface for presentation to CD4 T lymphocytes. Cell surface expression of MHC class II molecules loaded with peptide is strongly enhanced (10).

In contrast, the mechanism of MHC class I cross-presentation is less well characterized. In most studies presentation of exogenous antigen by MHC class I molecules was proteasome- and transporter associated with antigen processing (TAP)-dependent, indicating that peptides are generated in the cytosol and transported into the ER for MHC class I loading (11,12). It is not clear, however, how exogenous antigens gain access to the cytosol from the endocytic compartments. Substantial evidence supports involvement of components of the ER-associated degradation system (ERAD) in the translocation from the antigen-containing organelle into the cytosol (13-15). Alternatively, exogenously acquired antigen can also be processed and loaded in the endocytic track (16, 17).

We have now studied the longevity of MHC class I cross-presentation after highly effective receptor-mediated endocytosis of antigen by DCs. We observed storage of antigen for many days in a lysosome-like organelle, distinct from MHC class II compartments and different from the recently described early endosomal loading compartments (18, 19). The storage compartment described here serves as an antigen source for continuous supply of MHC class I ligands to sustain CD8 T cell cross-priming.

Materials and Methods

Mice, peptides and reagents

The animal experiments in this paper have been approved by the review board of Leiden University Medical Center. C57BL/6 mice were purchased from Charles River (St. Germain sur l'Arbresle, France). MHC class II knock-in mouse was kindly provided by M. Boes. Bone marrow derived from TAP1 deficient mice and TAP1/β2M deficient mice was kindly provided by B. Chambers (Karolinska Institute, Stockholm, Sweden). BM1 mice were obtained from The Jackson Laboratory (Mainz, USA). Synthetic peptides $OVA_{257-264}$ (OVA8, SIINFEKL), $OVA_{323-339}$ (OVA17, ISQAVHAAHAEINEAGR) and murine leukemia virus env-encoded T helper peptide (MuLV19, EPLTSLTPRCNTAWNRLKL) were synthesized in our laboratory. TLR ligand-long peptide conjugate containing the $OVA_{257-264}$ epitope is composed of Pam_3CysSK_4 covalently linked to the N-terminus of a 25-mer long peptide DEVSGLEQLESIINFEKLAAAAAK(4). Lipopolysaccharide (LPS) derived from E. Coli was obtained from Sigma.

Dendritic cells

Both bone marrow derived dendritic cells (BM DC) and the spleen derived D1 dendritic cell line (20, 35) were both used for all experiments except Fig. 1, 3, and 6 that were performed with D1 DCs.

Pulse-loading of dendritic cells with IgG-OVA complexes

IgG-OVA immune complexes (IgG-OVA) were made by incubating Ovalbumin (OVA, Worthington Biochemical Corporation) or OVA conjugated with Alexa Fluor 488 or Alexa Fluor 647 (Molecular Probes) with polyclonal rabbit anti-OVA IgG (ICN Biomedicals) for 30 min at 37°C in a mass ratio 1:50 as described (22). For pulse-loading, 10x concentrated IgG-OVA was added to medium and incubated for 1 or 2h at 37°C. To remove antigen, DCs were washed 3x with culture medium and subsequently cultured antigen-free for the period as indicated.

In vivo experiments

Priming of endogenous OVA-specific CTL in vivo was analyzed using SIINFEKL/K^b-tetramers labeled with APC (36). Cross-presentation of OVA in vivo was determined by using CFSE-labeled lymphocytes of OT-1 mice, transgenic for the TCR recognizing the OVA epitope SIINFEKL in H-2K^b.

Assessment of tumor protection capacity

Mice were challenged s.c. with 5 x 10^4 B16-OVA tumor cells two weeks after immunization. Mice were sacrificed when tumors had reached a volume of 1000 mm^3. Log-rank test was used for statistical analysis in Graph Pad Prism.

In vitro CD8 and CD4 T cell activation assay

CD8 T cell activation by DCs loaded with IgG-OVA, Pam3CysSK4-long peptide conjugate (23) or synthetic MHC class I-binding peptide $OVA_{257-264}$ (OVA8, SIINFEKL) in vitro was determined using B3Z T cell hybridoma (37). CD4 T cell activation by DCs loaded with Murine Leukemia Virus (MuLV) helper peptide (EPLTSLTPRCNTAWNRLKL) was determined by using 3A12-Z hybridoma (generated in our lab), specific for MuLV-derived peptide in I-A^b (38). Upon T cell activation they express β-galactosidase which can be measured by a colorimetric assay using 180 μg/ml chlorophenol red-beta-D-galactopyranoside (CPRG) as a substrate. Absorption is measured at 590 nm in a buffer containing 0.125% Nonidet P-40, 9 mM $MgCl_2$, and 100 mM β-mercapto-ethanol.

Mild acid elution of DC

DCs pulse-loaded with antigen were incubated for 90 sec with mild acid citrate/phosphate buffer (pH3.3) at RT to disrupt MHC class I/peptide complexes (26). Cells were either fixed in 0.2% PFA directly after elution or incubated in culture medium for recovery at 37°C and then fixed. In experiments with the proteasome inhibitor, cells were treated for 1h with 5μM epoxomicin before elution and during recovery.

SDS-PAGE

Cells were extensively washed with PBS to remove serum proteins. Next, the cell pellets were dissolved in sample buffer and boiled for 5 min at 95°C. Cell lysates of 2×10^5 cells were run on a 15% SDS-PAGE gel. Gels were scanned on the Typhoon Variable Mode Imager at an excitation wavelength of 488 nm (Amersham Bioscience).

Confocal scanning laser microscopy

DCs were transferred to glass bottom dishes (MatTek Corporation, Ashland, USA) 48h after pulse-incubation with IgG-$OVA^{Alexa488}$, fixed with 3.7% formaldehyde (Merck) and permeabilized with 0.5% saponin. DCs were subsequently incubated with antibodies (see below) for 30 min at 37°C in medium containing 0.1% saponin. In Fig. 5E, live BM DCs of the MHC class II eGFP knock-in mouse were cultured on glass bottom dishes, pulse-incubated with IgG-$OVA^{Alexa647}$ and imaged after 48h. The cells were imaged using an inverted Leica SP2 confocal microscope with a 63x objective lens. To avoid cross-excitation images were acquired by sequential scanning, with only one laser line per scan. Z-scan analysis was performed using 0.3 μm optical slices. For detailed images of high resolution, enabling visual judgement of co-localisation, single scan images were acquired in 5x magnification, displayed in Figure 5. Images were processed with ImageJ software.

The antibodies used for the confocal experiments described in Figures 5A to D were Alexa647 conjugated rat anti-mouse Lysosome-Associated Membrane Protein 1 (LAMP1) (Biolegend), goat anti-Early Endosomal Antigen 1 (EEA1) (Santa Cruz biotechnology), Cy™ 3 conjugated rabbit anti-goat IgG (Zymed®, Invitrogen), mouse anti-D^b (clone 28-14-8, BD Biosciences), Alexa647 conjugated goat anti-mouse Fab fragments (Invitrogen), goat anti-TAP1 (Santa Cruz biotechnology).

Confocal microscopy analysis

For co-localisation analysis Leica confocal software was used. For this purpose, the local intensity distribution of both fluorophores across a line scan drawn on a single optical slice was plotted in a graph (5). Co-localisation was scored from graphs of 30 eligible cells. Cells were eligible if intensity distribution of both fluorophores in the optical slice had an intensity distribution between 50 en 255 units. Co-localisation in the graphs was scored as either "no co-localisation", "minor co-localisation" or "major co-localisation".

Immuno-electron microscopy

Cryosections of D1 DCs were prepared as described (39) 48h after pulse-loaded with IgG-$OVA^{Alexa\ 488}$. Sections were immunogold double-labelled using specific antibodies against Alexa488, LAMP1, LAMP2, MHC class II or invariant chain (IC) with 10 and 15 nm gold particles as indicated.

Turnover of MHC class I and MHC class II

The cells were washed three times with ice cold PBS. 25x10e6 DCs were then incubated with 1 mg EZ-Link Sulfo-NHS-LC-Biotin (Pierce) in 1 ml PBS for 25 minutes at room temperature. After biotinylation, the DCs were washed three times with ice cold PBS, containing 100 mM glycine and further cultured in medium at 37 °C. At indicated time points, cells were lysed in lysis buffer (50mM Tris-HCl pH7.5, 5mM $MgCl_2$, 0.5% Triton X-100, 2 μg/ml aprotinin, 10 μg/ml leupeptin and 100μM PMSF) by three repeated freeze-thaw cycles in liquid nitrogen. Cell lysates were spun down at 13.000 RPM for 10 minutes at 4°C to remove intact cells and nuclei. Supernatants were pre-cleared with uncoated protein G sepharose beads (GE healthcare). Subsequently, supernatants were incubated with protein G sepharose beads pre-coated with antibodies specific for either MHC class I (clone B8243) or MHC class II (clone M5/114) for 1 hour at 4°C end-over-end. After extensive washing, the beads were added to sample buffer and boiled for 5 min at 95°C. Equal amounts of cell lysates were run on a 15% SDS-PAGE gel and proteins were transferred to a nitrocellulose membrane (Whatman). Blots were blocked O/N in PBS/0.1% Tween-20/5% milk and incubated for 2 hrs with SA-HRP in PBS/0.1% Tween-20. Blots were developed using enhanced chemiluminescence (Pierce) to assess the amount of biotinylated MHC class I and class II molecules during time. Tina software was used to assess intensity of the blot.

Results

Long lasting CTL priming capacity of dendritic cells after a short antigen pulse

To study kinetics of cross-presentation we used an antibody-mediated targeting system to deliver exogenous protein antigen to DCs. Antigen-specific IgG antibodies bind antigen with high affinity and are efficiently taken up by Fcγ receptors (20). Uptake of antibody-bound antigen by DCs is Fcγ receptor dependent (supporting information (SI) Fig. S1A). Endocytosis of antibody-bound Ovalbumin (IgG-OVA) by DCs is 1000-fold more efficient than uptake of free OVA as measured by flow cytometry with Alexa488-conjugated OVA (Fig. S1B). Targeting antigen via Fcγ receptors has two main advantages: very efficient uptake of the antigen and maturation of the DCs (21). Consequently, robust CTL responses can be induced by DCs loaded with antibody-bound antigen in submicromolar concentrations (20). To study the longevity of antigen presentation and priming capacity by DCs, we pulse-loaded DCs with antibody-bound antigen, washed the cells to remove free antigen and analyzed the kinetics of antigen presentation in MHC class I in vitro by co-culture with OVA-specific B3Z T cells. The optimal incubation time with IgG-OVA was assessed by pulse-incubations of different lengths. Pulse-incubation of 1 to 2h was already sufficient to induce optimal B3Z T cell activation comparable to 48h of continuous incubation (Fig. S1C). DCs pulse-loaded with irrelevant Ag-Ab complexes did not activate B3Z T cells, indicating that activation of B3Z is antigen dependent (Fig. S1D/E).

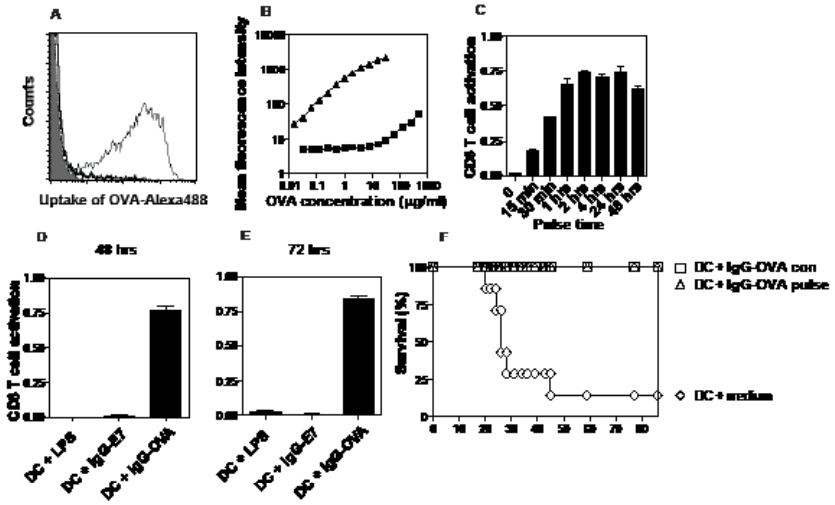

Supplementary Figure 1*:* (A) Uptake of IgG-OVA^{Alexa} by dendritic cells is FcγR dependent. BM DCs from wildtype (thin line) and FcR gamma chain deficient mice (black line) were pulse-loaded with IgG-OVA^{Alexa} for one hour and fluorescence was measured by FACS. Grey filled graph represents wildtype BM DC without IgG-OVA^{Alexa}. (B) Highly efficient uptake of IgG-OVA^{Alexa} (triangles) in comparison to free OVA^{Alexa} (squares) by dendritic cells. Mean fluorescence as measured by flow cytometry is depicted for each concentration of OVA either added free or bound by IgG. (C) Optimal CD8 T cell activation of IgG-OVA pulse-loading of DC is reached after one to two hours. DCs were pulse-loaded for indicated time with IgG-OVA. After incubation, IgG-OVA was washed away extensively and DCs were further cultured in medium. 48 hrs after the start of the antigen pulse CD8 T cell activation was assessed using B3Z hybridoma cells. Error bars represent SD of triplicates. (D/E) In vitro B3Z CD8 T cell activation by D1 dendritic cells at 48 hrs (D) or 72 hrs (E) after pulse-loading with either 10 µg/ml LPS, 1 µg/ml Human Papilloma Virus 16 E7 protein bound to specific IgG or 1 µg/ml OVA bound to specific IgG. (F) IgG-OVA pulsed DC can efficiently protect mice from a lethal B16-OVA melanoma tumor challenge. C57BL/6 mice (n=8) were immunized i.v. with DC pulse loaded with IgG-OVA followed by 48 hours culturing in the absence of IgG-OVA (DC + IgG-OVA pulse, squares); 48 hours continuous incubation with IgG-OVA (DC + IgG-OVA con, triangles); and incubated with medium (DC + medium, diamonds). % surviving mice is shown.

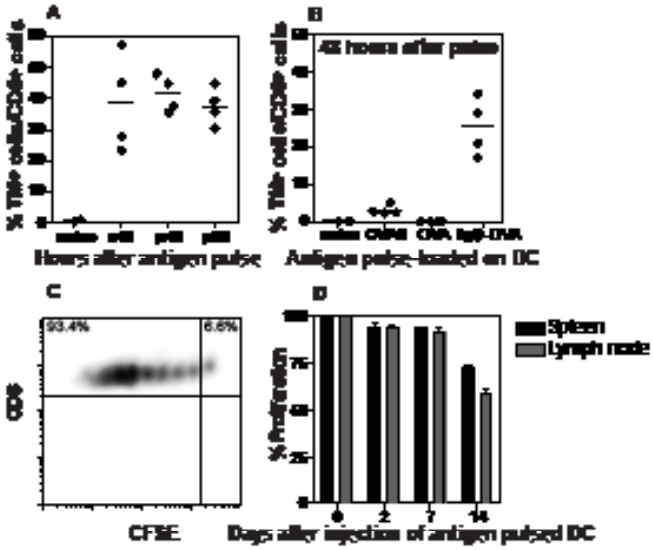

Fig. 1. Long lasting CTL priming capacity of dendritic cells after a short antigen pulse (A) Priming of OVA-specific CTL in mice that were injected i.v. with DCs continuously incubated with 1μg/ml IgG-OVA for 48h (c48); or pulse-incubated for one hour with 1μg/ml IgG-OVA and cultured for 48h (p48) or 96h (p96) in the absence of antigen. Each symbol represents the % tetramer (TM)-specific $CD8^+$ T cells from per mouse. (B) Priming of OVA-specific CTL in mice with matured DC 48h after pulse-loading with: 20nM of the minimal MHC class I binding peptide SIINFEKL (OVA8) + 10μg/ml LPS; 20nM OVA protein (OVA) + 10μg/ml LPS; or 20nM IgG-OVA.(C) In vivo proliferation of CFSE-labeled OVA-specific TCR transgenic $CD8^+$ T cells 2 days after i.v. injection of DCs that were pulse-incubated with 1μg/ml IgG-OVA. (D) In vivo T cell proliferation (as in C) in spleen (black bars) and lymph nodes (grey bars) at different days after i.v. injection of pulse-incubated DC.

To analyze the cross-priming potency of pulse-loaded DCs *in vivo*, naïve C57BL/6 mice were intravenously injected with DCs at 48 or 96h after antigen pulse-loading. In both groups of mice, high levels of OVA-specific $CD8^+$ T cells were observed, similar as in mice injected with DCs continuously incubated with IgG-OVA for 48h (Fig. 1A). In contrast, very inefficient priming of OVA-specific CTL was found when mice were vaccinated with mature DCs pulse-loaded with equimolar amounts of OVA protein or the minimal peptide (OVA8, SIINFEKL, Fig. 1B). These results show that IgG-OVA pulsed DCs have significantly prolonged cross-priming capacity *in vivo* compared to minimal peptide pulsed DCs. As a control using K^b mutant bm1 and TAP KO derived BM DCs, we showed that T cells were directly rather than indirectly primed by the injected DCs (Fig. S2).

Further we examined the longevity of cross-presentation *in vivo* to adoptively transferred CFSE-labelled naïve transgenic T cells that recognize the OVA8 peptide presented in MHC class I. T cell proliferation was analyzed in the spleen and lymph nodes by flow cytometry. Fig. 1C shows strong proliferation of CD8 T cells 48h after injection of DCs pulse-loaded with IgG-OVA. Strikingly, as long as 7 or 14 days after injection of pulse-loaded DCs, significant proliferation was observed (Fig. 1D).

We have previously reported that DCs continuously incubated with IgG-OVA for 48h fully protect mice in a CTL dependent fashion against a challenge with the lethal tumor cell line B16-OVA, an OVA-expressing melanoma (22). DCs pulse-loaded with IgG-OVA 48h before injection were fully effective in protecting mice challenged with B16-OVA (Fig. S1F). Importantly, this shows that long lived antigen presentation by mature DCs results in the induction of highly functional T cells *in vivo*.

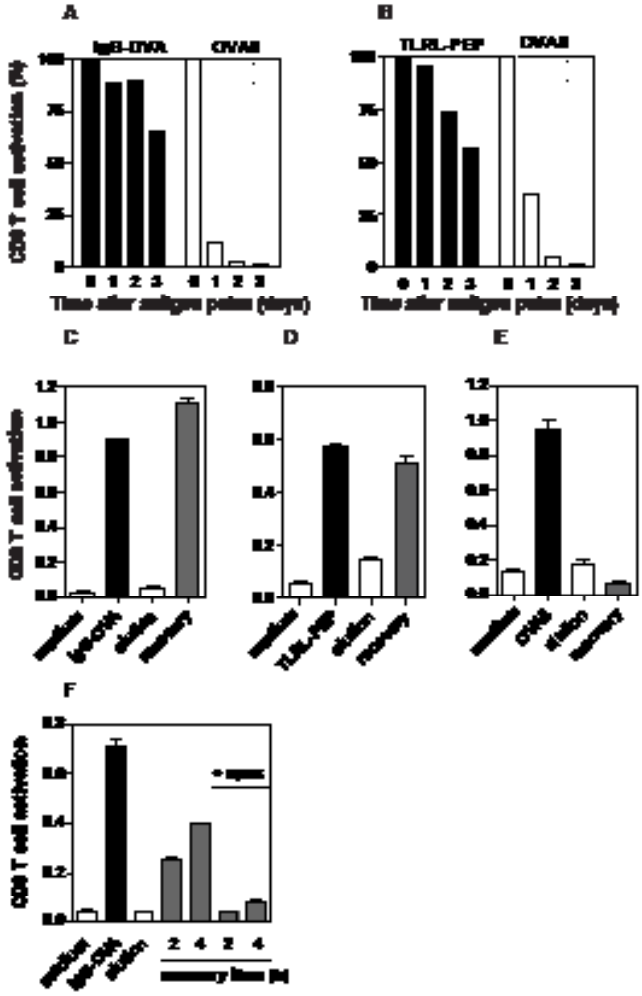

Fig. 2. Sustained MHC class I antigen presentation from an internal antigen source in DCs

(A/B) In vitro CD8$^+$ T cell activation DCs at subsequent days after pulse-incubation with 20nM IgG-OVA (A, black bars) or 0.5μM TLR ligand-long peptide conjugate (TLRL-PEP) (B, black bars), compared to equimolar amounts of OVA8 (white bars). Values depicted are relative to day 0. Experiment was repeated twice with similar results in both D1 DCs and BM DCs.

(C-E) In vitro CD8$^+$ T cell activation by DCs pulse-loaded with 10nM IgG-OVA (C); 0.5μM TLRL-PEP (D); or 10nM OVA8 (E). CD8$^+$ T cell activation was assessed 48h after pulse-loading with medium or the different compounds before (black bar) or after treatment with elution buffer (white bar) and after 16h recovery in the absence of antigen (grey bar). Error bars represent SD of triplicates. Experiments were performed 6x with similar results in both D1 DCs and BM DCs.

(F) CD8$^+$ T cell activation by DCs 48h after pulse-loading with medium or after pulse-loading with 10nM IgG-OVA with or without treatment with elution buffer and proteasome inhibitor epoxomicin. CD8$^+$ T cell activation was assessed directly after elution (white bar), or after 2h and 4h of recovery with or without 5mM epoxomicin. Experiment was performed 3x with similar results.

Instability of MHC class I/peptide complexes on cell surface of mature DCs

To investigate the mechanism of the sustained cross-priming capacity of DCs we analyzed the antigen presentation of pulse-loaded DCs *in vitro*. Antigen cross-presentation of antibody-bound OVA remained detectable for at least 3 days in contrast to presentation of pulse-loaded minimal MHC class I binding peptide, that was almost undetectable after 1 day (Fig. 2A). Similar results were obtained when we analyzed another efficient antigen targeting system: Toll like receptor 2-ligand Pam3CysSK4 conjugated to a long peptide containing the OVA CTL epitope SIINFEKL (23) (TLRL-PEP, Fig. 2B). Both antigen delivery systems have in common that the antigen needs intracellular processing, in contrast to the minimal MHC class I binding peptide that binds directly to MHC class I molecules at the cell surface. These results indicate that processing-dependent antigen, either protein or long peptide, is presented to CD8 T cells for a prolonged period.

The prolonged antigen presentation could be explained by the stability of the MHC class I/peptide complexes on the maturing DC. MHC class II/peptide complexes have been described as relatively stable at the cell surface of matured DCs (24, 25).

Therefore, we compared the stability of MHC class I and MHC class II/peptide complexes in DCs targeted with IgG-OVA leading to simultaneous maturation of the DC. 24h after the pulse-loading, all cell surface molecules of the DCs were labelled with biotin and further cultured. Cell samples were lysed at subsequent days and immune precipitation with MHC-specific antibodies was performed to assess the presence of biotinylated MHC class I and class II molecules. Strikingly, the majority of biotinylated MHC class I molecules had disappeared already after 24h while biotinylated MHC class II molecules were relatively stable; after 48h more than 50% still remained (Fig. 3A).

In parallel, we analyzed antigen presentation capacity of matured DCs pulse-loaded with minimal MHC class I and II binding peptides. We observed that antigen presentation to CD4 T cells was sustained significantly longer than antigen presentation to CD8 T cells (Fig. 3B). Together, these data indicate that MHC class I/peptide complexes, in contrast to MHC class II/peptide complexes, are relatively unstable at the cell surface of mature DC and have a high turnover. These data indicate that prolonged cross-presentation of IgG-OVA is not related to the stable presence of MHC class I/peptide complexes at the cell surface.

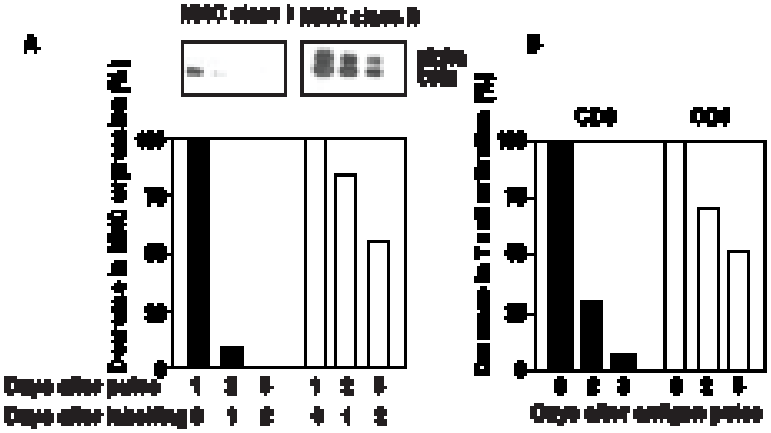

Sustained MHC class I cross-presentation from an internal antigen source

We further studied the long-lasting cross-presentation by disrupting MHC class I/peptide complexes at the cell surface by treatment with mild acid elution (26). DCs were pulse-loaded with IgG-OVA, TLR ligand-long peptide conjugate or the OVA8 minimal peptide. Mild acid elution of the live cells reduced MHC class I presentation to background levels (Fig. 2C-E). Importantly, 16h after elution, antigen presentation was recovered by IgG-OVA pulse-loaded DCs (Fig. 2C) and TLR ligand-long peptide conjugate-loaded DCs (Fig. 2D), but not by DCs pulsed with the OVA8 minimal peptide (Fig. 2E). The reappearance of MHC class I antigen presentation without renewed uptake of antigen indicates that the MHC class I ligands were derived from an internal antigen source. To examine if the recovery of MHC class I antigen presentation from the internal antigen source requires processing by the proteasome, DCs were treated with epoxomicin, a specific proteasome inhibitor, before and during recovery after mild acid elution. In untreated cells, CTL recognition was restored for more than 50% as early as 4h after elution. In cells treated with epoxomicin, recovery of MHC class I presentation was almost completely inhibited (Fig. 2F). In addition, in cells that lack the transporter associated with antigen presentation (TAP), as well as in cells that lack both TAP and β2M, initial presentation as well as recovery from the internal antigen source was not observed (Fig. S3A). Equal uptake of IgG-OVA complexes was verified using Alexa488-conjugated OVA (data not shown). Exogenous peptide loading of the minimal peptide SIINFEKL shows that the TAP deficient cells express sufficient MHC class I levels on the cell surface in contrast to cells that also lack the MHC class I light chain β2M (Fig. S3B). Taken together, these results indicate that processing of antigen from the newly identified intracellular source involves most likely a cytosolic proteasome and TAP-dependent pathway.

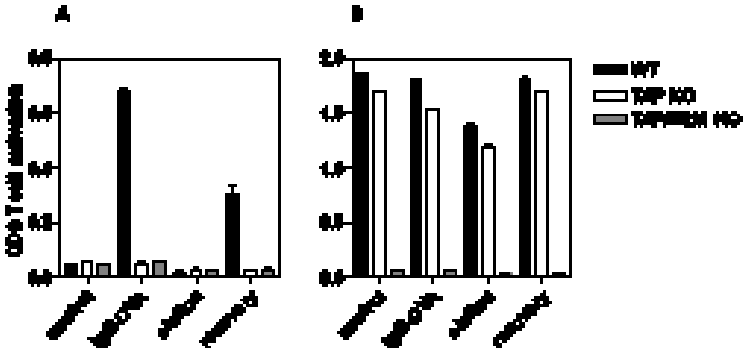

Supplementary Figure 3

(A) In vitro antigen presentation by BM DCs derived from wildtype (black bars, WT), TAP deficient mice (white bars, TAP KO), or TAP/β2M deficient mice (grey bars, TAP/β2M KO) 48 hours after pulse-loading with medium (control), 10 nM IgG-OVA before (IgG-OVA) or after (elution) treatment with elution buffer or after 6 hours of recovery in medium, as analyzed by activation of OVA-specific B3Z CD8 T cells. Error bar represents SD. (B) In vitro antigen presentation by BM DCs as in A, with extra 5 ng/ml minimal OVA peptide SIINFEKL added to each well during co-culture with B3Z CD8 T cells. Error bar represents SD.

Fig. 3, previous page. MHC class I-peptide complexes are short-lived on DCs compared to stable MHC class II-peptide complexes (A) Decrease of cell surface MHC class I (black bars) and β-chain of MHC class II (white bars) three consecutive days after biotinylation of D1 DCs which were pulse-loaded with IgG-OVA one day earlier. Upper panel: immuno-precipitated MHC class I and II molecules detected by Western blotting. This experiment was performed 2x with similar results. (B) Decrease of MHC class I and MHC class II antigen presentation by DCs pulse-incubated with minimal peptides. D1 DCs were pre-treated for 24h with 10μg/ml LPS and pulse-incubated for 2h with 100ng/ml MHC class I (OVA8, black bars) and 20μg/ml MHC class II binding peptides (MuLV19, white bars) at different days before analysis of specific T cell activation. Experiment was performed 2x with similar results.

Intracellular conservation of antigen after receptor-mediated uptake

To analyze the intracellular fate of antigen after receptor-mediated endocytosis, we pulse-loaded DCs with antibody-targeted OVA conjugated to Alexa488 (IgG-OVA^{Alexa}) and analyzed the cells at several time points by flow cytometry (Fig. 4A). Uptake of fluorescent OVA bound to IgG is very efficient, already after 1h strong fluorescence is detectable as shown previously (20) and in Figure S1A. After extensive washing the fluorescence signal still remained for several days. After 2 days 75 % of the fluorescence was detectable and diminished to about 50% after 4 days (Fig. 4A).

To analyze the nature of the antigen conserved in DCs, total cell lysates of DCs obtained at several time points after pulse-loading with IgG-OVA^{Alexa} were analysed by SDS-PAGE. Between 0 and 8h after antigen pulse, the original 45kD OVA band and a slightly smaller OVA product (approximately 40kD) were visible (Fig. S4). Subsequent days after the antigen pulse, the 40kD OVA species remained detectable in the cells that were pulse-loaded with IgG-OVA (Fig. 4B). This band was still present 7 days after pulse-loading with the antigen, indicating that the antigen was preserved for a long time (Fig. S4). In contrast, the antigen was not preserved in cells that were pulse-loaded with free OVA (Fig. 4B). The results of figure 2 and 4 together strongly indicate that DC preserve protein or long peptide antigen obtained via receptor-mediated uptake in an intracellular storage depot.

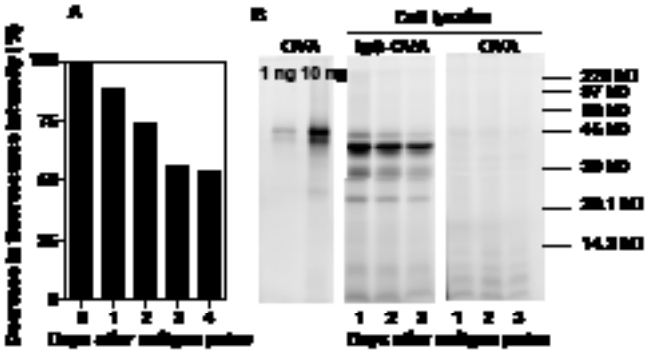

Fig. 4. Intracellular conservation of antigen after receptor-mediated uptake (A) Persistence of fluorescence in DCs at subsequent days after pulse-incubation with IgG-OVA^{Alexa488} as measured by flow cytometry. Experiment was performed 4x with similar results in both D1 DCs and BM DCs.(B) Persistence of OVA protein fragments in IgG-OVA^{Alexa488} pulse-loaded DCs determined by SDS-PAGE visualized directly in gel. Right lanes: total cell lysates of 2x10^5 DCs collected at subsequent days after pulse-loading. Left lanes: 1ng or 10ng of OVA^{Alexa488}. Experiment was performed 4x with similar results in both D1 DCs and BM DCs.

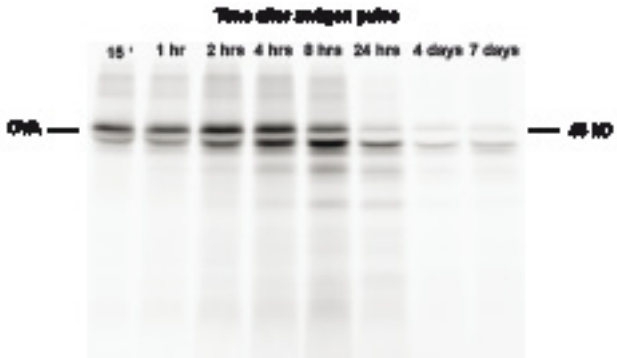

Supplementary Figure 4

Persistence of OVA protein fragments in IgG-OVA^{Alexa} pulse-loaded D1 dendritic cells determined by SDS-PAGE analysis visualized by direct in gel fluorescence. Lanes contain total cell lysates of 2x10^5 dendritic cells collected at different time points after the start of pulse-loading with 20 nM IgG-OVA^{Alexa}. This experiment was performed twice with similar results.

Antigen is conserved in storage organelles with lysosomal characteristics

To characterize the intracellular localisation of the antigen storage, we analysed DCs 48h after pulse-loading with IgG-OVA^{Alexa} using confocal microscopy. The fluorescence was localized in hotspots in the cytosol but not in the nucleus.We performed co-staining with antibodies to subcellular components and analyzed co-localisation with the Alexa positive compartments (Fig. 5). In all cells analyzed, the Alexa positive compartments co-localized to a large extent with lysosome associated membrane protein-1 (LAMP1) (Fig. 5A and Fig. S5D).

In contrast, in the majority of cells (70%) no co-localisation of Alexa positive compartments with the early endosomal antigen 1 (EEA1) was observed. In 30% of the cells, a minor proportion of the Alexa positive compartments co-localized with EEA1 (Fig. 5B and Fig. S5C). These results suggest that the antigen is localized in late endosomal or lysosomal compartments but not in early endosomal compartments or static endosomes. The latter were previously described as potential cross-presentation organelles (18, 19).

In addition, we tested the presence of MHC class I molecule K^b (Fig. 5C and Fig. S5A/B) and TAP (Fig. 5D and Fig. S5E) in the antigen containing storage organelles. Although some MHC class I positive hotspots could be observed intra-cellular, these hotspots did not co-localize with the antigen containing compartments in 90% of cells. In 10% of the cells, a minor fraction of the Alexa positive compartments was co-localized with MHC class I. In 60% of the cells, the Alexa positive compartments did not co-localize with TAP. However, in 40% of the DCs, some overlap could be observed between TAP and antigen containing organelles.

We next studied the presence of MHC class II in the antigen depots in living DC. Immature bone marrow derived DCs from MHC class II-eGFP knock-in mice were pulsed with IgG-OVA^{Alexa647}. After 48h virtually all detectable MHC class II was present at the cell surface of the matured DC (Fig. 5E and Fig. S5F). This is in line with increased cell surface expression and reduced intracellular expression of MHC class II after DC maturation (10, 25). In the same cells clear Alexa-positive intracellular hotspots were observed and therefore distinct from MHC class II loading compartments (MIIC).

To visualize the intracellular localization of the antigen storage depot in sub-cellular detail, we performed immuno-electron microscopy on DCs that were fixed 48h after pulse-loading with IgG-OVA^{Alexa}. Alexa 488-specific monoclonal antibodies were used to detect OVA^{Alexa} (Fig. 6A). OVA was mainly located in electron-dense, relatively large, spherical, membrane-delimited compartments. These compartments were negative for MHC class II (Fig. 6A), which was primarily located at the cell surface of the matured DCs. The OVA-enriched compartments were positive for LAMP1 (Fig. 6B) and LAMP2 (not shown) also indicating that the antigen was located in late endosomal or lysosomal compartments. The compartments were mono-vesicular and relatively electron dense, therefore structurally different from multi-vesicular MIIC and early endosomes. Moreover, the compartments did not label for invariant chain (IC) which is a marker for MIIC (Fig. 6C). In summary, the antigen storage organelles we now describe have a characteristic phenotype. They express lysosomal markers and are clearly distinct from MHC class I and MHC class II compartments.

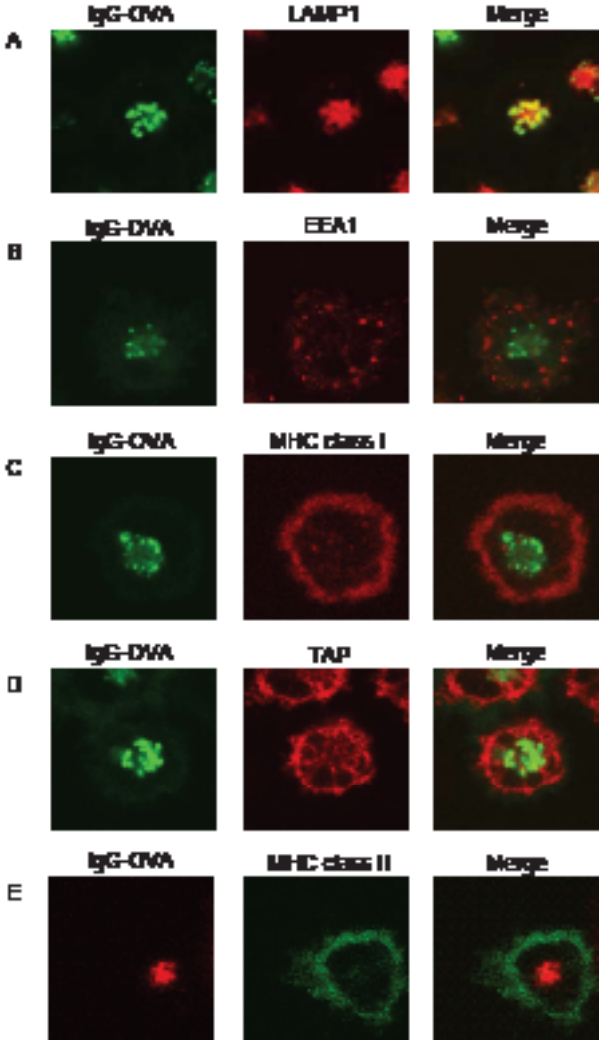

Fig. 5. Characterization of antigen containing compartments by confocal microscopy

(A-D) High resolution confocal images of DCs, 48h after pulse-incubation with IgG-OVA^{Alexa488}. Cells were fixed, permeabilized and incubated with Abs specific for LAMP1 (A) and EEA1 (B), MHC class I (C) and TAP1 (D). Single scans are representative for multiple cells analyzed in at least 2 experiments. Both D1 DCs and BM DCs were used. (E) Confocal images of BM DCs derived from the MHC class II-eGFP knock-in mouse 48h after pulse-incubation with IgG-OVA^{Alexa647}.

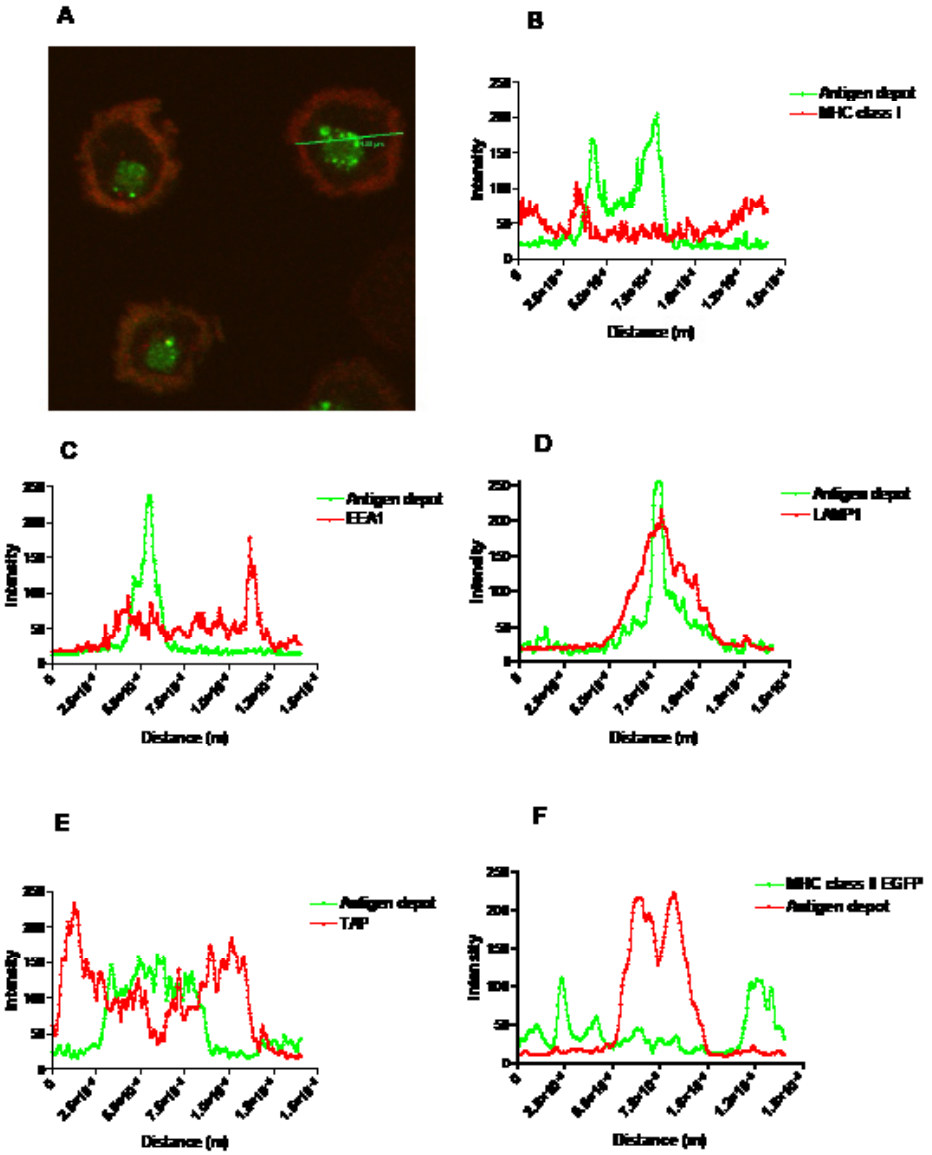

Supplementary Figure 5

(A) Example of a line scan for quantification of co-localisation obtained with Leica confocal software.

(B-E) Intensity profiles of Alexa488^{+} antigen depot (green) and red: K^{b} (B), EEA1 (C), LAMP1 (D), TAP (E) across line scan. One representative example of at least 30 cells analyzed is shown.

(F) Intensity profile of MHC class II/eGFP (green) and Alexa647^{+} antigen depot (red) across line scan.

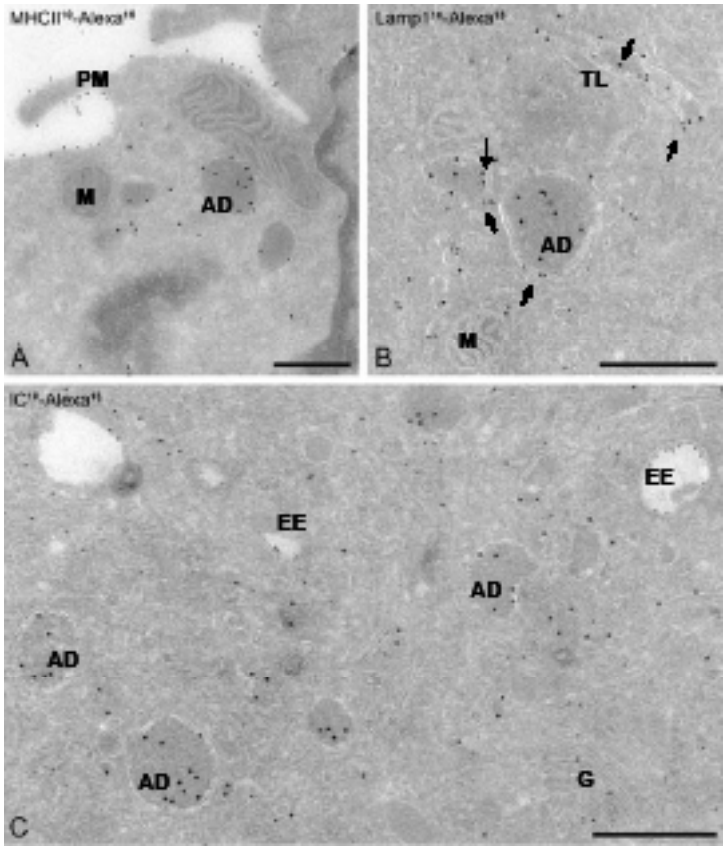

Fig. 6. Antigen storage organelles are electron dense with lysosomal characteristics (A-C) Immuno-electron microscopy images of D1 DCs at 48h after pulse-loading with IgG-OVA^{Alexa488}. Sections were double-immunogold labelled for MHC class II (A), LAMP1 (B), invariant chain (IC) (C), and Alexa488 (A-C) with gold particle sizes as indicated in nm. Asterisks indicate antigen depots (AD), arrow heads indicate LAMP-1. PM=plasma membrane, M=mitochondrion, EE=early endosome, G=Golgi complex. Scale bar = 200 nm.

Discussion

Our main salient finding is that DCs can conserve protein antigen in intracellular depots for many days, associated with continuous MHC class I presentation. DCs with intracellular stored antigen can prime high numbers of specific $CD8^+$ T cells in vivo that were fully effective in CTL-mediated tumor control. We characterized the storage organelles as lysosome-like compartments that can mediate maintenance of MHC class I cross-presentation. These structures are clearly distinct form the recently described early endosomal loading compartments allowing rapid MHC class I presentation (18, 19). This reveals division of labour between distinct specialized compartments in DCs. It appears that specialized APCs utilize different organelles to organize antigen handling internalized via different receptor systems. Here, we target low doses of protein antigen to DCs via Fc receptors, which is 1000-fold more efficient than e.g. mannose receptor mediated uptake (Fig. S1B).

Our gel electrophoretic analysis shows that fragments of the OVA protein antigen are stably conserved in DCs (Fig. 4 and Fig. S4). Delamarre and co-workers have shown that DCs have a quantitatively and qualitatively different content of lysosomal enzymes than macrophages, relating to efficiency of MHC class II presentation (27). In addition, it has been reported that endosomes in DCs are actively alkalized by NOX2, creating an environment unfavourable for lysosomal proteases (28). Thus, these data support our findings that DC can retain antigen for prolonged periods of time in specialized organelles. The crucial novelty of our study is that the conservation of protein antigen in DC is related to prolonged MHC class I presentation.

The depot formation described here was studied in two different systems of receptor-mediated uptake: IgG-antigen and TLR ligand-long peptide conjugates (Fig. 2). Both modes of presentation combine efficient targeting of antigen to the DC and a DC maturation signal in one compound and are therefore attractive vaccine formulations. This combination leads to a more efficient priming capacity compared to long peptides not conjugated to TLR ligand (23) or OVA not bound to IgG (20). The efficient targeting and maturation in one compound might be a requirement for the depot formation. Indeed, we could not induce depot formation when we pulse-loaded DCs with free OVA or OVA peptide even when combined with a separate TLR ligand. Both formulations used in this study contain antigen that requires intracellular processing to release the MHC class I ligand(s). The proteasome is the most important enzyme system responsible for the degradation of protein antigens. We have previously described that the proteasome activator PA28 is strongly up-regulated after stimulation with IgG-OVA, CD40 stimulation or TLR triggering of DCs (29). This indicates that maturing DCs can increase their antigen processing mechanisms as well as enhance their co-stimulatory capacity. Together, these two mechanisms favor optimal continuous presentation of antigenic peptides derived from the antigen depots to T cells.

We have observed that recovery of cross-presentation after peptide elution was proteasome-dependent (Fig. 2F). The antigen may reach the proteasome when it is translocated from the storage compartments into the cytosol as described for antibody-bound antigen (12). After proteasomal degradation, the antigen may follow the classical ER located MHC class I presentation pathway, since we have observed that FcγR-dependent cross-presentation and recovery after elution is TAP-dependent (Fig. S3). However, treatment with brefeldin A, an inhibitor of protein secretion, and treatment with cycloheximide, an inhibitor of protein synthesis, only marginally affected recovery after elution (data not shown). These data would argue against the ER as the site of MHC class I loading and leaves space for an alternative route. Fusion of components of the ER-associated degradation system (ERAD) with antigen containing compartment has been described (13-15). In this study, we did not find evidence in support of such an ER-antigen fusion compartment, because the majority of antigen depots lacks the presence of TAP and

MHC class I molecule K^b. Therefore, we conclude that the antigen containing organelles are storage depots but not MHC class I loading compartments. We can not exclude the involvement of distinct MHC class I loading compartments, possibly containing recycling MHC class I from the cell surface (16, 17). The intracellular MHC class I hotspots we observed in close proximity to the antigen containing compartments (Fig. 5C and Fig. S5A/B) and the fast recovery of antigen presentation after elution may support this hypothesis. Therefore we propose that the antigen-containing organelle described here is an antigen storage compartment rather than an MHC class I processing/loading compartment.

In Fig. 3, we show that cell surface-expressed MHC class I molecules have a significantly shorter half life than MHC class II molecules on mature DCs. This correlates with different kinetics of presentation of exogenously loaded antigenic peptides to CD8 and CD4 T cells. Whereas MHC class II-peptide complexes are stable for several days, most MHC class I-peptide complexes disappear from the cell surface within 24h. The kinetics of MHC class I molecule turnover are important for biological function in immune surveillance by CD8 T cells. MHC class I molecules display an up-to-date overview of the internal content of the cell; they continuously present ligands derived from cytosolic proteins, newly synthesized misfolded proteins or viral proteins (8). However, without a continuous supply route, this high turnover of peptide-MHC complexes does not favor cross-priming of $CD8^+$ T cells. Professional antigen-presenting cells such as DCs engulf the antigen in the periphery and travel to the T cell zones in lymphoid organs without encountering a new source of exogenous antigen (30). This migration time has been estimated to last 24-48h (31, 33). At the time of arrival, the number of cognate peptide/MHC class I complexes in the immunological synapse need to be above a threshold to ensure effective contacts between DCs and T cells (33). Thus, DCs require the important function of exogenous antigen storage to ensure continuous generation of MHC class I ligands for presentation to CD8 T cells. We have shown that mature DCs have a long term capacity to prime antigen-specific $CD8^+$ T cells in vivo (Fig. 1).

The minimal binding peptide we have used in this study, SIINFEKL, has a very high affinity for MHC class I (34), yet we observed that the T cell priming capacity of DCs pulsed with this peptide is less effective and less sustained than that of DCs pulsed with antibody-bound protein or long peptide. We propose that this difference is mediated by the depot formation described in the current study. Our data indicate that antigen targeting to internal depots, where the antigen is conserved, may improve the effectiveness of vaccines. Therefore, vaccine formulations composed of targeted protein or long peptides leading to long lived cross-priming capacity of DCs are to be favored over vaccine formulations composed of minimal peptides that are rapidly lost from MHC class I molecules, which are often used in vaccination and DC-based adoptive transfer trials nowadays.

Footnotes

Author contributions: NvM, SK, JSV, HJG, CJM and FO designed research and analyzed data. NvM, SK, MGC and JMG performed research. DVF, JJW and TvH contributed reagents. NvM, JSV, CJM and FO wrote the paper.

Acknowledgements

We would like C. Franken for the production of tetramers.

This work was supported by grant UL 2004-3008 from the Dutch Cancer Society (to NvM and MGC), a MTC grant from The Netherlands Organisation for Scientific Research (NWO) (to SK and DVF) and a grant from the European Community: DC-Thera (to FO).

References

1. Melief C J (2003) Mini-review: Regulation of cytotoxic T lymphocyte responses by dendritic cells: peaceful coexistence of cross-priming and direct priming? *Eur. J. Immunol.* 33:2645-2654.

2. Shen L, Rock K L (2006) Priming of T cells by exogenous antigen cross-presented on MHC class I molecules. *Curr. Opin. Immunol.* 18:85-91.

3. Bevan M J (2006) Cross-priming. *Nat. Immunol.* 7:363-365.

4. Banchereau J, Steinman R M (1998) Dendritic cells and the control of immunity. *Nature* 392:245-252.

5. Guermonprez P, Valladeau J, Zitvogel L, Thery C, Amigorena S (2002) Antigen presentation and T cell stimulation by dendritic cells. *Annu. Rev. Immunol.* 20:621-667.

6. Schuurhuis D H, Fu N, Ossendorp F, Melief C J (2006) Ins and outs of dendritic cells. *Int. Arch. Allergy Immunol.* 140:53-72.

7. Tacken P J, de Vries I J, Torensma R, Figdor C G (2007) Dendritic-cell immunotherapy: from ex vivo loading to in vivo targeting. *Nat. Rev. Immunol.* 7:790-802.

8. Yewdell J W (2007) Plumbing the sources of endogenous MHC class I peptide ligands. *Curr. Opin. Immunol.* 19:79-86.

9. Turley S J *et al* (2000) Transport of peptide-MHC class II complexes in developing dendritic cells. *Science* 288:522-527.

10. Kleijmeer M *et al* (2001) Reorganization of multivesicular bodies regulates MHC class II antigen presentation by dendritic cells. *J. Cell Biol.* 155:53-63.

11. Groothuis T A, Neefjes J (2005) The many roads to cross-presentation. *J. Exp. Med.* 202:1313-1318.

12. Rodriguez A, Regnault A, Kleijmeer M, Ricciardi-Castagnoli P, Amigorena S (1999) Selective transport of internalized antigens to the cytosol for MHC class I presentation in dendritic cells. *Nat. Cell Biol.* 1:362-368.

13. Guermonprez P *et al* (2003) ER-phagosome fusion defines an MHC class I cross-presentation compartment in dendritic cells. *Nature* 425:397-402.

14. Houde M *et al.* (2003) Phagosomes are competent organelles for antigen cross-presentation. *Nature* 425:402-406.

15. Ackerman A L, Giodini A, Cresswell P (2006) A role for the endoplasmic reticulum protein retrotranslocation machinery during crosspresentation by dendritic cells. *Immunity.* 25:607-617.

16. Kleijmeer M J *et al* (2001) Antigen loading of MHC class I molecules in the endocytic tract. *Traffic.* 2:124-137.

17. Gromme M *et al* (1999) Recycling MHC class I molecules and endosomal peptide loading. *Proc. Natl. Acad. Sci. U. S. A* 96:10326-10331.

18. Burgdorf S, Kautz A, Bohnert V, Knolle P A, Kurts C (2007) Distinct pathways of antigen uptake and intracellular routing in CD4 and CD8 T cell activation. *Science* 316:612-616.

19. Burgdorf S, Scholz C, Kautz A, Tampe R, Kurts C (2008) Spatial and mechanistic separation of cross-presentation and endogenous antigen presentation. *Nat. Immunol.* 9:558-566.

20. Schuurhuis D H *et al* (2002) Antigen-antibody immune complexes empower dendritic cells to efficiently prime specific CD8+ CTL responses in vivo. *J. Immunol.* 168:2240-2246.

21. Regnault A *et al* (1999) Fcgamma receptor-mediated induction of dendritic cell maturation and major histocompatibility complex class I-restricted antigen presentation after immune complex internalization. *J. Exp. Med.* 189:371-380.

22. Schuurhuis D H *et al* (2006) Immune complex-loaded dendritic cells are superior to soluble immune complexes as antitumor vaccine. *J. Immunol.* 176:4573-4580.

23. Khan S *et al* (2007) Distinct uptake mechanisms but similar intracellular processing of two different toll-like receptor ligand-peptide conjugates in dendritic cells. *J. Biol. Chem.* 282:21145-21159.

24. Cella M, Engering A, Pinet V, Pieters J, Lanzavecchia A (1997) Inflammatory stimuli induce accumulation of MHC class II complexes on dendritic cells. *Nature* 388:782-787.

25. Wilson N S, El Sukkari D, Villadangos J A (2004) Dendritic cells constitutively present self antigens in their immature state in vivo and regulate antigen presentation by controlling the rates of MHC class II synthesis and endocytosis. *Blood* 103:2187-2195.

26. Storkus W J, Zeh H J III, Salter R D, Lotze M T (1993) Identification of T-cell epitopes: rapid isolation of class I-presented peptides from viable cells by mild acid elution. *J. Immunother.* 14:94-103.

27. Delamarre L, Pack M, Chang H, Mellman I, Trombetta E S (2005) Differential lysosomal proteolysis in antigen-presenting cells determines antigen fate. *Science* 307:1630-1634.

28. Savina A *et al* (2006) NOX2 controls phagosomal pH to regulate antigen processing during crosspresentation by dendritic cells. *Cell* 126:205-218.

29. Ossendorp F *et al* (2005) Differential expression regulation of the alpha and beta subunits of the PA28 proteasome activator in mature dendritic cells. *J. Immunol.* 174:7815-7822.

30. Garg S *et al* (2003) Genetic tagging shows increased frequency and longevity of antigen-presenting, skin-derived dendritic cells in vivo. *Nat. Immunol.* 4:907-912.

31. Itano A A, Jenkins M K (2003) Antigen presentation to naive CD4 T cells in the lymph node. *Nat. Immunol.* 4:733-739.

32. MartIn-Fontecha A *et al* (2003) Regulation of dendritic cell migration to the draining lymph node: impact on T lymphocyte traffic and priming. *J. Exp. Med.* 198:615-621.

33. Henrickson S E *et al* (2008) T cell sensing of antigen dose governs interactive behavior with dendritic cells and sets a threshold for T cell activation. *Nat. Immunol.* 9:282-291.

34. Lipford G B, Bauer S, Wagner H, Heeg K (1995) In vivo CTL induction with point-substituted ovalbumin peptides: immunogenicity correlates with peptide-induced MHC class I stability. *Vaccine* 13:313-320.

35. Winzler C *et al* (1997) Maturation stages of mouse dendritic cells in growth factor-dependent long-term cultures. *J. Exp. Med.* 185:317-328.

36. Schuurhuis D H *et al* (2000) Immature dendritic cells acquire CD8(+) cytotoxic T lymphocyte priming capacity upon activation by T helper cell-independent or -dependent stimuli. *J. Exp. Med.* 192:145-150.

37. Sanderson S, Shastri N (1994) LacZ inducible, antigen/MHC-specific T cell hybrids. *Int. Immunol.* 6:369-376.

38. Ossendorp F, Mengede E, Camps M, Filius R, Melief C J (1998) Specific T helper cell requirement for optimal induction of cytotoxic T lymphocytes against major histocompatibility complex class II negative tumors. *J. Exp. Med.* 187:693-702.

39. Geuze H J, Slot J W, van der Ley P A, Scheffer R C (1981) Use of colloidal gold particles in double-labeling immunoelectron microscopy of ultrathin frozen tissue sections. *J. Cell Biol.* 89:653-665.